Original Research

Normobaric hyperoxia inhibits the progression of lung cancer by inducing apoptosis

Sei Won Kim[1], In Kyoung Kim[1], Jick Hwan Ha[2], Chang Dong Yeo[3], Hyeon Hui Kang[1], Jin Woo Kim[3] and Sang Haak Lee[1,4]

[1]Division of Pulmonary, Critical Care and Sleep Medicine, Department of Internal Medicine, St. Paul's Hospital, College of Medicine, The Catholic University of Korea, Seoul 02559, Republic of Korea; [2]Division of Pulmonary and Critical Care Medicine, Department of Internal Medicine, Incheon St. Mary's Hospital, College of Medicine, The Catholic University of Korea, Incheon 21431, Republic of Korea; [3]Division of Pulmonary and Critical Care Medicine, Department of Internal Medicine, Uijeongbu St. Mary's Hospital, College of Medicine, The Catholic University of Korea, Uijeongbu 11765, Republic of Korea; [4]Cancer Research Institute, College of Medicine, The Catholic University of Korea, Seoul 06591, Republic of Korea

Corresponding author: Sang Haak Lee. Email: mdlee@catholic.ac.kr

Impact statement

Normobaric hyperoxia (NBO) is a feasible therapy for cancer with a low complication rate. Although NBO may be beneficial in cancer treatment, very few studies have been conducted; thus, the evidence is thin. This is the first study to clearly demonstrate morphological changes in lung cancer with NBO exposure and to investigate the underlying mechanisms both *in vivo* and *in vitro*. This study will arouse interest in NBO treatment and promote further research.

Abstract

Hypoxia is a critical characteristic of solid tumors with respect to cancer cell survival, angiogenesis, and metastasis. Hyperoxic treatment has been attempted to reverse hypoxia by enhancing the amount of dissolved oxygen in the plasma. In this study, we evaluated the effects of normobaric hyperoxia on the progression of lung cancer to determine whether oxygen toxicity can be used in cancer therapy. Following a tail vein injection of the Lewis lung carcinoma cells, C57BL/6J mice were exposed to a 24-h normobaric hyperoxia/normoxia cycle for two weeks. In addition, A549 lung cancer cells were incubated in a normobaric hyperoxia chamber for a 24-h period. As a result, the size and number of tumors in the lung decreased significantly with exposure to normobaric hyperoxia in the mouse model. Cell viability, colony-forming ability, migration, and invasion all decreased significantly in A549 cells exposed to normobaric hyperoxia and the normal control group exposed to normobaric hyperoxia showed no significant damage. Oxidative stress was more prominent with exposure to normobaric hyperoxia in cancer cells. A549 cells exposed to normobaric hyperoxia showed a significantly higher cell apoptosis ratio compared with A549 cells without normobaric hyperoxia exposure and normal human lung cells (BEAS-2B cells). The Bax/Bcl-2 mRNA expression ratio also increased significantly. Changes in the key regulators of apoptosis were similar between *in vivo* and *in vitro* conditions. The p-ERK level decreased, while the p-JNK level increased, after normobaric hyperoxia exposure in A549 cells. This study demonstrated the role of normobaric hyperoxia in inhibiting lung cancer. Normal tissue and cells showed no significant hyperoxic damage in our experimental setting. The anti-tumor effect of normobaric hyperoxia may due to the increased reactive oxygen species activity and apoptosis, which is related to the mitogen-activated protein kinase pathway.

Keywords: Lung neoplasms, hyperoxia, reactive oxygen species, oxidative stress, apoptosis, mitogen-activated protein kinase signaling system

***Experimental Biology and Medicine* 2018; 243: 739–748. DOI: 10.1177/1535370218774737**

Introduction

Hypoxia commonly occurs in solid tumors as a result of an inadequate supply of oxygen, due to rapid cancer growth and an insufficient vascular supply.[1] Hypoxia has been proven to promote cancer growth and treatment resistance.[1–5] Under a hypoxic environment, tumor cells adapt

by inducing angiogenesis and altering their metabolism, via increased glycolysis and upregulation of genes involved in cell survival/apoptosis.[1,6–8]

To delay cancer progression and improve therapeutic efficacy, recent studies have focused on eliminating the hypoxic state in tumors.[2,3,9,10] Hyperbaric oxygen (HBO) treatment, which can increase the oxygen content in various tissues, has been applied in many studies seeking to reverse the hypoxic condition.[2,3,5,10,11] Mouse studies using HBO treatment showed favorable outcomes, such as retardation of tumor growth and increased treatment efficacy.[2,5,9,10] However, HBO treatment can also present some complications, including barotraumatic lesions, oxygen toxicity, confinement anxiety, and ocular effects.[12,13] High oxygen concentrations may also be toxic to the central nervous system.[14]

Another method of hyperoxic treatment is normobaric hyperoxia (NBO), which is an attractive alternative to HBO due to its ease of administration and non-invasiveness.[15] NBO treatment has been actively investigated in patients suffering from acute ischemic stroke, and its benefits have been demonstrated in several studies.[16–19] However, to date, very few reports have found a beneficial effect of NBO in lung cancer. In this study, we evaluated the effects of NBO on the progression of lung cancer both *in vivo* and *in vitro*. Several indicators related to tumor growth, oxidative stress, and apoptosis were measured to identify the mechanisms underlying the effects of NBO treatment.

Materials and methods

Experimental design and NBO treatment

Male C57BL/6J mice (7–8 weeks old) were purchased from DBL (Chungcheongbuk-do, Korea). The Lewis lung carcinoma (LLC) cell line was obtained from the American Type Culture Collection (ATCC, Manassas, VA, USA) and injected at 5×10^5 cells/mouse through the tail vein. Immediately after LLC cell injection, mice were placed within their cages in a Plexiglass chamber, in which an atmosphere of 95% O_2 was constantly monitored using an oxygen analyzer (BioSpherix Ltd, Redfield, NY, USA). The temperature within the chamber was maintained at $22 \pm 1°C$ and the relative humidity was $60 \pm 5\%$. Mice were exposed to a 24-h NBO/normoxia cycle for two weeks and weighed weekly during the experiment. Controls were exposed to normoxia for the identical time frame. All animal experimental protocols were approved by the Animal Subjects Committees of the Catholic University of Korea (SPH-20100813–004).

Lung tumor analysis

The gross morphology and number of lung tumor nodules were recorded after sacrificing the mice. Size was measured with Thorpe calipers, and tumor volume was calculated using the formula: $(d^1 \times d^2 \times d^3) \times 0.5236$, where d^n represents the three orthogonal diameters. The lung tissues were inflated and fixed by 10% formalin at 25 cmH_2O pressure prior to histological analysis. Hematoxylin and eosin (H&E)-stained slides of tumor tissues were scanned with a Panoramic MIDI slide scanner (3DHISTECH Ltd, Budapest, Hungary).

Mean linear intercept

Mean linear (Lm) was assessed in 10 non-overlapping fields of lung parenchyma per animal at 200× magnification. A transparent sheet with 10 equally distributed horizontal lines is laid over the printed digitized image of an H&E-stained section and the intercepts with the tissue structures are counted. The total length of the grid lines was then divided by the number of intersections to provide the mean linear intercept in micrometer.

Bronchoalveolar lavage fluid sampling

Immediately after blood collection, bronchoalveolar lavage (BAL) fluid was collected by lavage of the lung through the trachea. The trachea was cannulated with silicone tubing attached to a 23-gauge needle on a tuberculin syringe. The total number of cells in the BAL fluid was counted using a hemocytometer. The BAL fluid was cytospined (5 min at $750 \times g$) and stained with Diff-Quick (Sysmex, Tokyo, Japan) for differential counts. The cells were differentiated into macrophages, lymphocytes, neutrophils, and eosinophils by general leukocyte morphology. The percentage of each cell type was calculated by counting 500 leukocytes on randomly selected regions of the slides under a light microscope.

TUNEL assay

Apoptotic cell deaths in sections of mouse lungs were detected by TUNEL assay using an in situ apoptosis detection kit (Promega, Madison, WI, USA) as instructed by the manufacturer. Briefly, 4-μm-thick sections of paraffin-embedded tissue were deparaffinized and hydrated in graded alcohol solutions. After incubating with a proteinase K and washing in PBS, equilibration buffer and terminal deoxynucleotidyl transferase were added to all slides followed by incubation at 37°C for 1 h. The slides were immersed in saline sodium citrate and counterstained, followed by several washes with distilled water. On the slides, lung cells with brown nuclear labeling were considered as TUNEL positive. Staining was evaluated using Olympus light microscope under 200× magnification.

Cell culture and morphological observations

A549 (human alveolar adenocarcinoma) cells and BEAS-2B (human bronchial epithelial cells) were obtained from the ATCC. Control cells were incubated in room air, whereas cells in the hyperoxia-exposure group were incubated in a hypoxia chamber (Oxycycler; BioSpherix, Parish, NY, USA) with an 85% O_2/5% CO_2 gas mixture for 24 h. Cell morphological changes were observed and photographed under a phase-contrast inverted microscope (TS-100F, Nikon, Tokyo, Japan).

Cell viability assay

Cell viability was determined by the 3–(4,5-dimethylthiazol-2-yl)-2,5 diphenyltetrazolium bromide (MTT) assay. Cells were cultured for 24 h and then exposed to an 85% O_2 condition for 24 h. Then, the MTT solution was added and incubated for 4 h at 37°C. The purple formazan was dissolved in dimethyl sulfoxide (DMSO) and absorbance was measured at 570 nm. Cell viability was calculated as the percentage of absorbance of cells in the hyperoxia group compared with that of cells in the control group.

Lactate dehydrogenase activity

Lactate dehydrogenase (LDH) activity was evaluated spectrophotometrically in the culture media after exposure to hyperoxia using an LDH cytotoxicity kit according to the manufacturer's instructions. LDH release was determined as the percentage of LDH in medium compared with the total LDH in each well using the following equation: (test sample – low control)/(high control – low control) × 100.

Colony-forming ability assay

The colony formation assay was performed as described previously.[20] Briefly, after exposure to hyperoxia, the cells were re-plated in a six-well plate in complete culture medium under room air. After 14 days, the colonies that formed were stained with a crystal violet cell stain solution (Cell Biolabs, San Diego, CA, USA).

Wound-healing and invasion assay

Cell migration was determined by a scratch wound-healing motility assay. Cells were cultured for 24 h and then exposed to the 85% O_2 condition for 24 h. After the exposure, cells were cultured in complete medium to a nearly confluent cell monolayer. The cell monolayer was scratched to create a linear ''wound'' 1 mm in width. A defined area of the wound was photographed using the phase-contrast inverted microscope before exposure to hyperoxia. After exposure, the cells that migrated into the zero line of the linear "wound" were identified by image analysis. Cell invasive ability was examined by the Transwell migration assay. A Transwell membrane (8-um pore size) coated with Matrigel was used. After exposure to hyperoxia, the cells were seeded in the Matrigel-coated upper wells. After a 24-h incubation, the cells that had invaded the lower surface were stained with crystal violet.

Reverse transcription polymerase chain reaction

Total RNA was extracted from lung tissue or cells using TRIzol (Invitrogen, Carlsbad, CA, USA). First-strand cDNA was synthesized from total RNA using the Super Script II first-strand synthesis system (Invitrogen). Quantitative real-time polymerase chain reaction (PCR) was performed with the QuantiFast SYBR Green PCR kit (Qiagen, Valencia, CA, USA). The threshold cycle (Ct) value for each gene was normalized to the Ct value of β-actin. Relative mRNA expression was calculated using the $2^{-\Delta\Delta CT}$ method. Semi-quantitative RT-PCR amplification was performed using caspase-3/-9, p53, Bax, Bcl-2, and β-actin primers. The PCR reaction was started at 94°C for 5 min, followed by 25–30 cycles at 94°C for 30 s at the annealing temperature of each primer, 72°C for 30 s, and a final extension step at 72°C for 10 min. Equal volumes of PCR product were separated by 2% agarose gel electrophoresis.

Western blotting and zymography

Cells were cultured for 24 h and then exposed to the 85% O_2 condition for 24 h. Equal amounts of extracted total cell protein (30 μg/sample) were separated using 8–15% sodium dodecyl sulfate-polyacrylamide gel electrophoresis (SDS-PAGE) and then transferred to poly(vinylidene) fluoride (PVDF) membranes. The membranes were blocked with 5% skim milk and incubated at 4°C overnight with a 1:1000 dilution of anti-Bax, anti-Bcl2, anti-caspase-3/-9, anti-poly (ADP-ribose) polymerase (PARP), anti-p53, anti-extracellular regulated kinase (ERK), anti- c-Jun N-terminal kinase (JNK), and anti-β-actin antibody (Cell Signaling Technology, Danvers, MA, USA). After washing, the membranes were incubated with secondary antibody for 2 h. The signals were detected using an enhanced chemiluminescence Western blot detection kit and visualized by exposure to X-ray film. Collagenolytic activity in hyperoxia-exposed cells was measured by gelatin zymography and 8% SDS-PAGE containing 0.1% gelatin. After electrophoresis, the gels were washed with 2.5% Triton X-100 followed by an overnight incubation at 37°C in zymography reaction buffer. The gels were stained with Coomassie Brilliant Blue R-250 and then destained.

Flow cytometry

Progression of the cell cycle, apoptosis, and intracellular reactive oxygen species (ROS) levels were assessed with the Muse™ Cell Analyzer (Merck-Millipore, Darmstadt, Germany) according to the manufacturer's instructions. The cells were cultured for 24 h and then exposed to the 85% O_2 condition for 24 h. The cell cycle analysis was carried out using the Muse® Cell Cycle kit (Merck-Millipore). Apoptosis was measured using Muse™ Annexin-V and the Dead Cell kit (Merck-Millipore). Intracellular ROS generation was measured by the dichlorofluorescein diacetate (DCF-DA) method using the Muse® Oxidative Stress kit (Merck-Millipore).

Enzyme-linked immunosorbent assay

The concentrations of albumin (Abcam, Cambridge, UK), superoxide dismutase (SOD) (Dojindo Laboratories, Rockville, MD, USA), myeloperoxidase (MPO), the ratio of reduced glutathione (GSH)/oxidized glutathione (GSSG), and lipid peroxidation (MDA) (Bioassay Systems, Hayward, CA, USA) were measured in BAL fluid or tissue lysate with ELISA kits, according to the manufacturer's instructions.

Statistical analysis

All data are expressed as means ± standard deviations. Statistical comparisons between groups were performed using the parametric independent *t*-test if the dependent variable was continuous and had a normal distribution. Otherwise, the Mann–Whitney *U* test was used. A *P*-value <0.05 was considered significant. All statistical analyses were performed GraphPad Prism software (ver. 5.0 for Windows; GraphPad Software, La Jolla, CA, USA).

Results

Tumor growth inhibition and histological changes in vivo

Figure 1(a) shows the H&E-stained histopathological lung tissue sections in the normal and LLC-bearing mouse groups. No significant morphological changes were detected in the lung tissue of the normal mice exposed to hyperoxia. The lung tumors were histologically classified as hyperplasia, adenoma, or adenocarcinoma based on previously established criteria.[21] The LLC-induced lung tumors were histologically classified as lung adenomas or adenocarcinomas. Importantly, the histological analyses demonstrated that multiple large tumor nodules were evident in the LLC control group, whereas the number and size of nodules in the 24 h hyperoxia-exposed LLC group decreased significantly compared with those in the LLC control group (both $P < 0.01$). However, no significant morphological changes were observed in the normal lung region of the LLC-bearing mouse groups following hyperoxia exposure, as in the control groups. Results on tumor incidence and total tumor volume in the LLC mouse group are illustrated in Figure 1(b) and (c). To find the effects of hyperoxia on normal lung tissue, airspace size was estimated by mean linear intercept in normal mouse group (Figure 1(d)). There was no significant difference of mean linear intercept with 24 h NBO treatment in normal mouse group. Mean body weight during the two weeks did not differ between the groups (data not shown).

Effect of NBO on inflammation, antioxidative enzyme activities, and apoptosis in vivo

The total number of inflammatory cells was counted in BAL fluid from mice in each group to quantify the inflammatory response. Although the numbers of neutrophils and lymphocytes tended to increase slightly after 24 h of hyperoxia in both the normal and LLC mouse groups, no significant differences were observed (Figure 2(a)). The total numbers of cells and macrophages increased significantly in the 24 h hyperoxia-exposed LLC group compared with those in the LLC control group (both $P < 0.001$). Albumin in BAL fluid

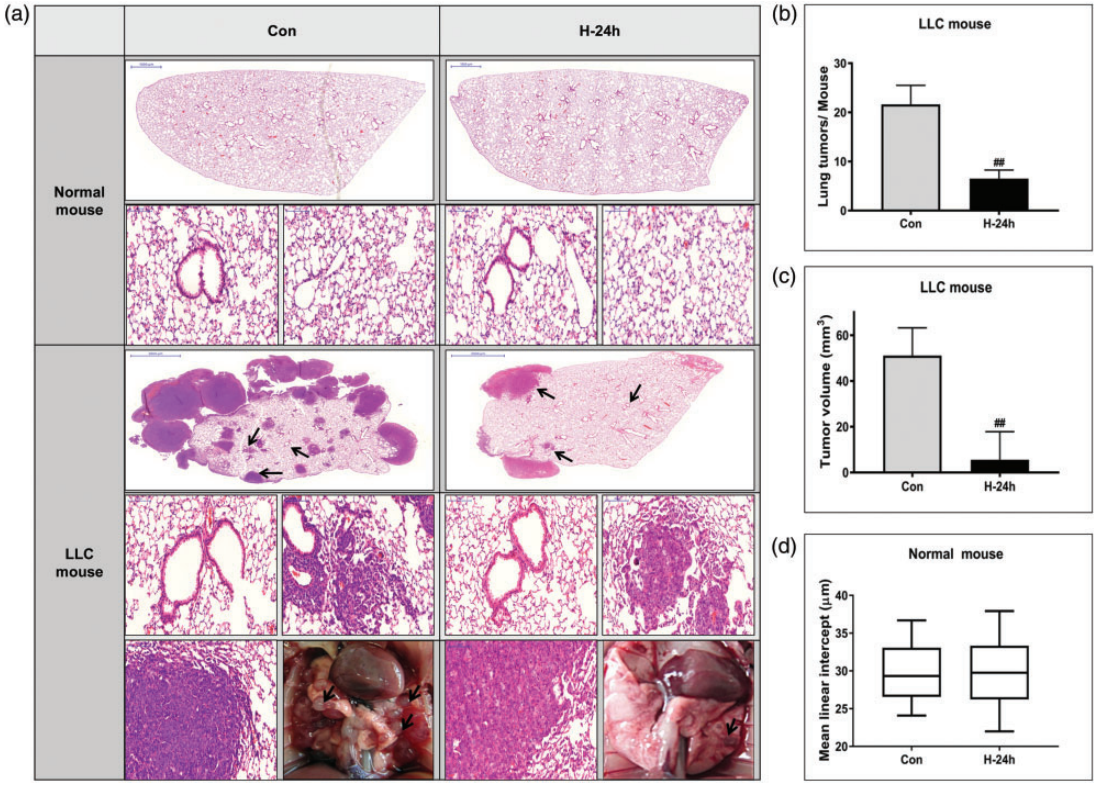

Figure 1. Tumor growth inhibition and histological changes *in vivo*. (a) Photographs of the dissected tumors and representative images of hematoxylin and eosin (H&E)-stained lung sections. The two top panels show images of whole lung sections and higher magnification of the same samples (magnification, ×400) in normal mice. The three bottom panels show images of whole lung section, higher magnification of the rectangle in the whole lung section (magnification, ×400) and gross lung examination in Lewis lung carcinoma (LLC) mice. Lung tumors are indicated by arrows in the gross lung examination at the bottom panel. Lung tumor development was evaluated according to (b) the size and number of tumors in each group at the study endpoint and (c) tumor volume. (d) Airspace size was estimated by determining the mean linear intercept in normal mouse. The data represent the mean ± SD. $^{\#\#}P < 0.01$ compared with LLC + NBO, 0 h. (A color version of this figure is available in the online journal.)

was measured as a marker of pulmonary epithelial permeability changes and lung damage to identify the occurrence of hyperoxia-induced toxicity (Figure 2(b)). The albumin level in the LLC group tended to be higher than that in the normal group, but the difference was not significant. No significant difference in the effect of hyperoxic treatment was observed between the normal and LLC mouse groups. In addition, the activity of MPO as a proinflammatory enzyme was measured in lung tissue (Figure 2(c)). The MPO level decreased significantly after the hyperoxic treatment in the LLC mouse group ($P < 0.05$). However, no difference was observed in the normal mouse group.

We investigated whether exposure to hyperoxia affects the activity of pulmonary enzymes usually involved in antioxidant defense. The level of SOD in lung homogenate was not different between the study groups (Figure 2(d)). The ratio of GSH/GSSG, which represents consumption of GSH resulting from the accumulation of ROS, decreased significantly after hyperoxia in both groups (both $P < 0.05$, Figure 2(e)). The MDA level in lung homogenates tended to increase with exposure to the hyperoxic treatment in both groups (Figure 2(f)). We determined whether exposure to hyperoxia can play an anti-tumor role by activating the mitochondrial-dependent apoptosis signaling pathway. Total Bax and cleaved caspase-3 protein levels, as direct evidence of increased apoptosis, increased in the hyperoxia-exposed LLC mice group, whereas the Bcl-2 protein level decreased (Figure 2(g)). The real-time RT-PCR results showed a significant increase in the Bax/Bcl-2 mRNA ratio compared with that in the control group of LLC-bearing mice ($P < 0.01$, Figure 2(h)). In addition, hyperoxia-exposed LLC mice group showed more TUNEL-positive lung cancer cells than control group (Figure 2(i)).

Effect of NBO on cell morphological changes and growth inhibition in vitro

The microscopic image of A549 cells after 24 h of hyperoxia revealed a pleomorphic appearance with atypical nuclei and numerous mitotic figures (Figure 3(a)). In contrast, BEAS-2B cells showed a conserved cell pattern after 24 h of hyperoxia. Cell toxicity increased significantly in both BEAS-2B and A549 cells ($P < 0.01$ and $P < 0.001$, respectively, Figure 3(c)). Colony-forming ability decreased significantly in BEAS-2B and A549 cells ($P < 0.05$ and $P < 0.01$, respectively, Figure 3(d) and (e)). However, A549 cells tended to show more toxicity and less colony-forming ability after hyperoxia exposure compared with those of BEAS-2B cells. In addition, only A549 cells showed a significant decrease in cell viability after the 24 h hyperoxia exposure ($P < 0.001$, Figure 3(b)).

NBO inhibits lung cancer cell migration and invasion in vitro

The wound-healing and Matrigel cell invasion assays were performed to evaluate the ability of NBO to inhibit cell migration and invasion. Cell migration and invasion decreased in both assays after the 24 h hyperoxia exposure of A549 cells (Figure 4(a) and (b)). Quantification of the

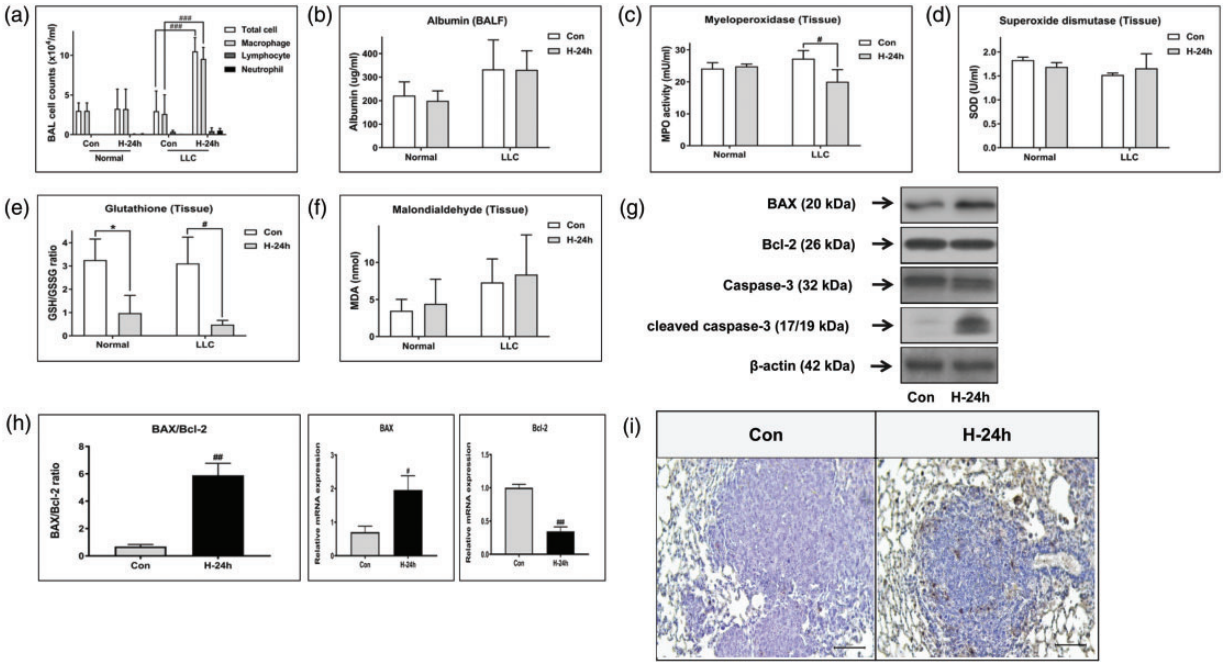

Figure 2. Effect of NBO on inflammation, antioxidant enzyme activities and apoptosis *in vivo*. (a) Total and differential cells in bronchoalveolar lavage (BAL) fluid. The levels of (b) albumin and (c) myeloperoxidase (MPO) were measured as indicators of inflammation and lung injury in BAL fluid and lung tissue, respectively. The levels of (d) superoxide dismutase (SOD), (e) the ratio of reduced glutathione (GSH)/oxidized glutathione (GSSG), and (f) lipid peroxidation (MDA), as indicators of oxidative stress, were measured in the total lung homogenate. (g) The expression of apoptosis-related genes, such as caspase-3, Bax, and Bcl-2, was examined in total protein by Western blotting. (h) Bax and Bcl-2 mRNA expression was examined by real-time polymerase chain reaction. (i) TUNEL-stained lung sections from control and NBO-treated Lewis lung carcinoma (LLC) mice are shown. $^{\#}P < 0.05$, $^{\#\#}P < 0.01$ and $^{\#\#\#}P < 0.001$ compared with LLC + NBO, 0 h. $^{*}P < 0.05$ compared with control + NBO, 0 h. (A color version of this figure is available in the online journal.)

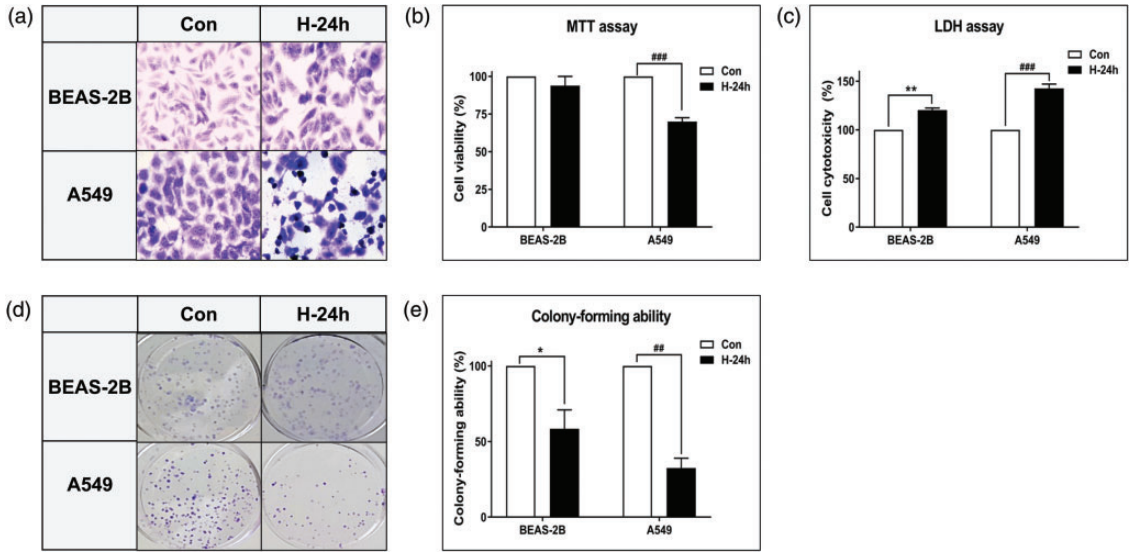

Figure 3. Effect of NBO on morphological changes and growth inhibition *in vitro*. (a) Cells were stained with Wright and Giemsa (original magnification 400×). After the hyperoxic treatment, A549 cells had a pleomorphic appearance with atypical nuclei and numerous mitotic figures. Comparison of (b) cell viability and (c) cell toxicity after exposure to hyperoxia in BEAS-2B and A549 cells. Cell viability and toxicity after 24 h hyperoxia exposure were expressed as a percentage of untreated control samples. (d) Colony growth ability. Immediately after exposure to hyperoxia, the cells were re-plated in a six-well plate at a density of 500 cells. The cells were then cultured for 7–14 days in a room-air incubator, and cell colonies were stained. (e) The formed colonies were quantified. Data represent the mean ± SD number of colonies as a percentage of untreated control samples. These results are representative of three independent experiments. $^{*}P < 0.05$ and $^{**}P < 0.01$ compared with BEAS-2B + NBO, 0 h. $^{\#\#}P < 0.01$ and $^{\#\#\#}P < 0.001$ compared with A549 + NBO, 0 h. (A color version of this figure is available in the online journal.)

migrated and invaded cells showed the same results (both $P < 0.001$, Figure 4(c) and (d)). We also measured matrix metalloproteinase (MMP)-9 and MMP-2, which are associated with tumor migration and invasion. A549 cells showed decreased levels of MMP-9 and MMP-2 after the 24 h hyperoxia exposure (Figure 4(e)).

Effect of NBO on ROS, cell cycle distribution, and apoptosis

Relative ROS levels increased significantly in A549 cells after 24 h of hyperoxia exposure ($P < 0.01$), whereas BEAS-2B cells showed no significant changes (Figure 5(a)). The percentage of cells in the G0/G1 phase decreased significantly in BEAS-2B and A549 cells after hyperoxia exposure (both $P < 0.001$, Figure 5(b)). However, the cell apoptosis ratio was significantly higher after 24 h of hyperoxia exposure only in A549 cells ($P < 0.05$, Figure 5(c))

Effect of NBO on apoptosis and MAPK signaling pathways

The expression of apoptosis- and cell survival-related genes, such as PARP, caspases, p53, p21, Bax, and Bcl-2, were examined for mRNA and total protein (Figure 6(a) and (b)). The mRNA expression of caspase-3, caspase-9, Bax, and p53 tended to increase after hyperoxia exposure. The protein levels of cPARP, cleaved caspase-9, cleaved caspase-3, Bax, p-p53, and p21 also increased in A549 cells after hyperoxia exposure. In contrast, Bcl-2 decreased in both mRNA expression and protein level after hyperoxia exposure. To ascertain if there was a role for the MAPK pathway in hyperoxia-induced apoptosis, the expression levels of proteins such as ERK and JNK were examined (Figure 6(c)). Phosphorylation of ERK decreased in A549 cells with 24 h hyperoxia exposure. In contrast, p-JNK increased after 24 h hyperoxia exposure.

Discussion

We demonstrated that NBO inhibits the growth of lung cancer. Cell viability, colony-forming ability, migration, and invasion all decreased in cancer cells treated with NBO. In addition, the normal group exposed to NBO developed no significant damage. Our results also suggest that the antitumor effect of NBO may be due to increased ROS activity and apoptosis, which is related to the MAPK pathway. To date, very few studies have investigated NBO and lung cancer. This is the first study to clearly demonstrate morphological changes in lung cancer with NBO exposure, and to investigate the mechanisms underlying this effect.

Hypoxia is a critical characteristic of solid tumors and involves enhanced cancer cell survival, angiogenesis, and metastasis.[2,22] Hypoxia also reduces the sensitivity of cancer to radiotherapy or chemotherapy.[23] To delay cancer progression and improve therapeutic efficacy, recent studies have focused on eliminating the hypoxic state in tumors.[3,9,24] HBO treatment, which can increase oxygen content in various tissues, has been attempted and showed favorable results in terms of inhibition of tumor growth and increased treatment efficacy.[2,3,5,10,11] Although HBO induces a higher oxygen concentration in tumor tissues than NBO, herein we used NBO because it is a more feasible therapy with a lower complication rate in actual clinical practice.[12–14] In addition, both normobaric

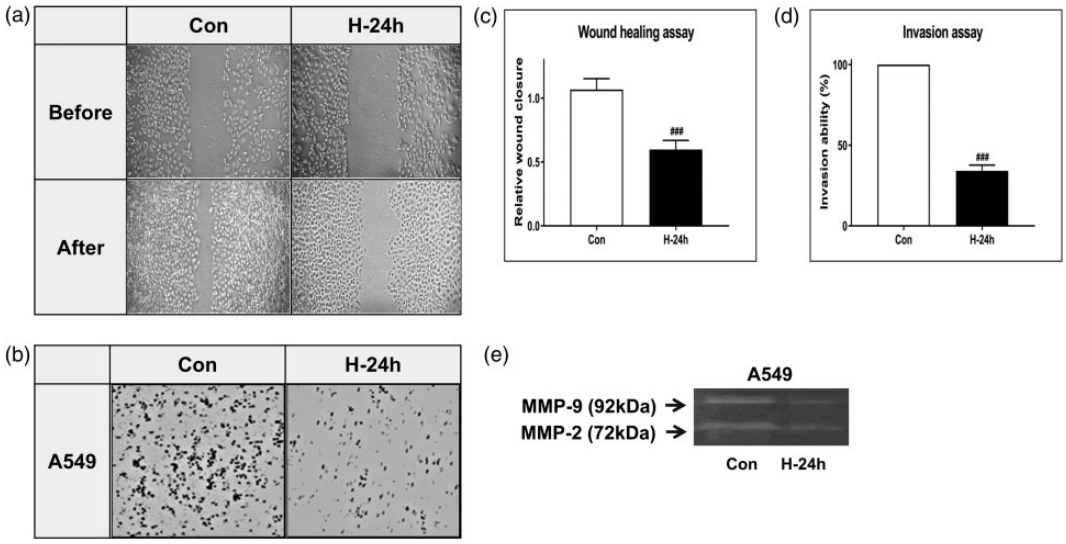

Figure 4. NBO inhibits lung cancer cell migration and invasion. (a) The wound-healing assay was used to detect the migration ability of A549 cells. Representative photographs showing the same area at 0 h and after 24 h of hyperoxia (85% O_2) exposure. (b) The Matrigel assay was used to detect the invasion ability of A549 cells. Random fields were scanned for the presence of cells on the lower side of the membrane. (c) Migrated cells and (d) Matrigel invaded cells were quantified. Data represent the mean ± SD. $^{###}P < 0.001$ compared with A549 + NBO, 0 h. (e) Gelatin zymography analysis for matrix metalloproteinase (MMP)-2 and MMP-9. After 24 h of hyperoxia (85% O_2), the cells were subjected to gelatin zymography to investigate the MMP-2/-9 activity. Triplicate experiments were performed.

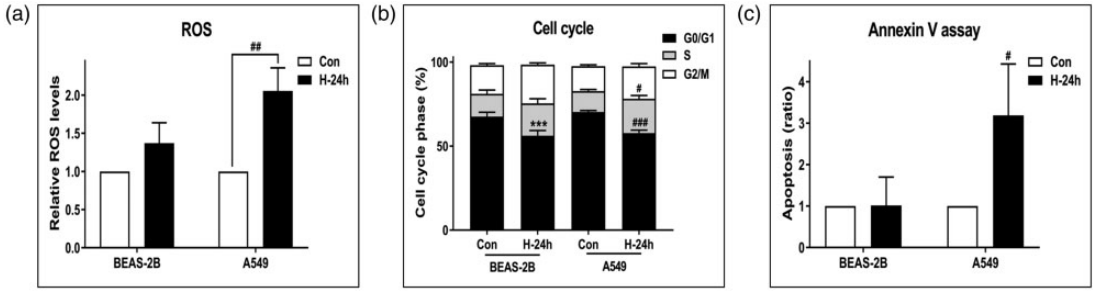

Figure 5. Effect of NBO on reactive oxygen species (ROS), cell cycle distribution, and apoptosis. Cells were treated with room air or hyperoxia (85% O_2) for 24 h. Then, cells were analyzed for (a) ROS (b), cell cycle distribution, and (c) apoptosis using the Muse™ Cell Analyzer. The amount of ROS was measured according to dichlorofluorescein diacetate (DCFH-DA) intensity. Cell populations at the G1, S, and G2/M phases were determined using the Muse® Cell Cycle kit. Apoptosis was performed by the method of Kloesch *et al*. (with slight modifications) using the Muse® Annexin-V and Dead Cell kit. Error bars represent the standard deviation, and each result was determined as the average of three independent experiments. $^{***}P < 0.001$ compared with BEAS-2B + NBO, 0 h. $^{#}P < 0.05$, $^{##}P < 0.01$ and $^{###}P < 0.001$ compared with A549 + NBO, 0 h.

and hyperbaric hyperoxia significantly retarded tumor growth in other mouse studies.[5,25] However, to date, few studies have compared NBO and HBO.

Prolonged exposure to hyperoxia can cause injury to normal lung tissue.[26] Hyperoxic lung injury in experimental animals represents an established model of acute respiratory distress syndrome.[13] In this study, we applied 95% O_2 *in vivo* and 85% O_2 *in vitro*, consistently for 24 h. Our preliminary study revealed that the number of inflammatory cells increased significantly after continual exposure to hyperoxia for 48 h or more, with lung injury beginning to appear when hyperoxia exposure was continuous for over 72 h (data not shown). Under our experimental setting (NBO for 24 h), the normal mouse group, and normal tissues adjacent to the tumor in the cancer group, showed no definite histological damage. No changes in various inflammatory cell counts were detected in the BAL fluid of the normal mouse group. Total cell and macrophage counts increased significantly in LLC-bearing mice exposed to NBO. However, the lymphocyte and neutrophil counts did not change significantly, and the MPO level decreased rather than increased. Overall, 24 h of NBO did not produce any significant histological damage or inflammation in either the normal or cancer group.

Oxidant/antioxidant homeostasis is highly regulated and essential for maintaining cellular and biochemical functions.[27] Production of excessive free oxygen radicals beyond endogenous antioxidant capacity can lead to oxidative damage.[28] The major antioxidants of the lungs are SODs, catalase, and GSH-associated enzymes.[29,30] Here, we considered endogenous antioxidant enzyme and MDA activities as indicators of oxidative stress. Although SOD and MDA did not change significantly in response to hyperoxia *in vivo*, the GSH/GSSG ratio decreased significantly after hyperoxia in both the normal and cancer mouse group. In addition, ROS increased significantly only in

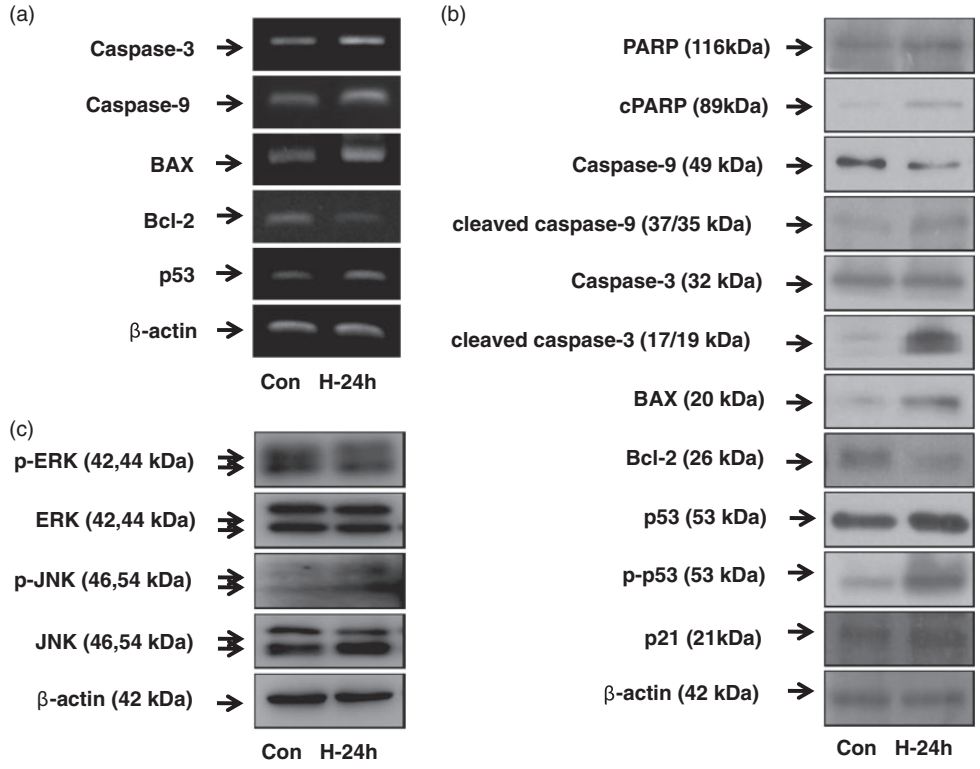

Figure 6. Effect of NBO on apoptosis and mitogen-activated protein kinase (MAPK) signaling pathways. Cells were treated with room air or hyperoxia (85% O_2) for 24 h. Then, A549 cells were harvested and RNA was isolated using Trizol. (a) mRNA expression of caspase-3, -9, Bax, Bcl-2 and p53 was examined by reverse transcription polymerase chain reaction (RT-PCR). PCR products were resolved on a 2% agarose gel. (b) The expression levels of apoptosis and cell survival-related genes, such as poly (ADP-ribose) polymerase (PARP), caspases, p53, p21, Bax and Bcl-2 were examined in total protein by Western blotting. (c) Protein levels of extracellular regulated kinase (ERK) and c-Jun N-terminal kinase (JNK) were examined in total protein by Western blotting.

A549 cells after 24 h of hyperoxia. This result suggests that oxidative stress is more prominent in cancer tissue exposed to hyperoxia compared with normal tissue exposed to hyperoxia. It has long been postulated that cancer cells balance high ROS levels and increased antioxidant ability compared with normal cells.[31] In this situation, increasing oxidative stress above the toxicity threshold induces cancer cell death while sparing normal cells, which are characterized by lower intracellular ROS levels.[32] Many chemotherapeutic agents, including taxanes, vinca alkaloids, and platinum-based agents, are currently used to induce high ROS levels, resulting in cell death.[33] Increased ROS plays an important role in the induction of apoptosis.[34,35] Ott *et al.*[36] showed that ROS play an important role in the release of cytochrome *c* and other pro-apoptotic proteins, which can activate caspases and apoptosis.[36] We investigated whether exposure to hyperoxia plays an anti-tumor role by activating the mitochondrial-dependent apoptosis signaling pathway. Anti-apoptotic factor Bcl-2 decreased significantly, and pro-apoptotic factor Bax increased significantly, in the LLC mouse group exposed to hyperoxia. The Bax/Bcl-2 ratio, which regulates apoptosis by modulating outer mitochondrial membrane permeability,[37] also increased significantly in our study. Cleaved caspase-3, which is the key factor in the activation of caspases during apoptosis, also increased. A549 cells exposed to hyperoxia had a significantly higher cell apoptosis ratio compared with those of BEAS-2B cells and A549 cells that were not exposed to hyperoxia. In addition, changes in the key regulators involved in apoptosis showed the same trend as the *in vivo* study. Overall, the present study revealed that NBO induced apoptosis in cancer.

To identify the mechanism linking increased ROS levels and apoptosis, we investigated MAPK pathways, mediated by ERK and JNK, which are well known to modulate cell survival and proliferation.[38] ERK is important for cell survival and is activated in response to growth stimuli in cancer.[39] In contrast, JNK is generally activated by stress and is closely associated with cell death.[40] In accordance with previous reports, the level of p-ERK decreased, while that of p-JNK increased, after NBO in our study. Makena *et al.*[41] also showed that prolonged exposure to hyperoxia and a high tidal volume induces ROS-mediated activation of JNK and apoptosis. We also attempted to identify the relationship between apoptosis and cell cycle arrest. The cell cycle is regulated by multiple control points at different phases; failure of these control points can lead to abnormal growth or apoptosis.[42] Our results showed a significantly lower frequency of G0/G1 phases after NBO in both BEAS-2B and A549 cells. However, this cell cycle arrest was not cancer-specific and we did not find a further relationship with apoptosis.

We are aware of the limitations of this study. First, NBO treatment time cycle in our study is incomplete and needs

more research to find more relevant, non-toxic protocols. Although we tried to find the appropriate treatment time from preliminary studies, variety of time cycles can be possible. Second, normal tissue damage with 24 h NBO treatment was not significant in this study. However, more precise analysis about the safety is still needed. Third, the beneficial effects of NBO treatment should be investigated with concurrent chemotherapy and radiotherapy. Finally, therapeutic effects of NBO in this study rely on mouse model and cell study. Applying NBO treatment to human directly is difficult yet. More clinical investigations for human are needed.

In conclusion, the present study showed the role of NBO in inhibiting lung cancer. Exposing cancer cells to NBO resulted in increased ROS activity, which triggered apoptosis via the MAPK pathway. Normal tissue and cells showed no significant hyperoxic damage in our experimental setting. Further research could reinforce the use of NBO in the clinical setting for lung cancer treatment with minimal lung injury.

Authors' contributions: SWK managed the overall experiment and wrote the manuscript. IKK conducted the experiments and analyzed the data. JHH, CDY, and HHK participated in the interpretation of the studies and manuscript editing. JWK and SHL supervised the project. All authors read and approved the final manuscript.

DECLARATION OF CONFLICTING INTERESTS

The author(s) declared no potential conflicts of interest with respect to the research, authorship, and/or publication of this article.

FUNDING

The author(s) disclosed receipt of the following financial support for the research, authorship, and/or publication of this article: This research was supported by Basic Science Research Program through the National Research Foundation of Korea (NRF) funded by the Ministry of Education (2014R1A1A2058026) and by grants Clinical Research Laboratory of The Catholic University of Korea, St. Paul's Hospital.

ORCID iD

Sei Won Kim http://orcid.org/0000-0002-2798-421X

REFERENCES

1. Shannon AM, Bouchier-Hayes DJ, Condron CM, Toomey D. Tumour hypoxia, chemotherapeutic resistance and hypoxia-related therapies. *Cancer Treat Rev* 2003;**29**:297–307
2. Moen I, Stuhr LE. Hyperbaric oxygen therapy and cancer – a review. *Targ Oncol* 2012;**7**:233–42
3. Doguchi H, Saio M, Kuniyoshi S, Matsuzaki A, Yoshimi N. The enhancing effects of hyperbaric oxygen on mouse skin carcinogenesis. *J Toxicol Pathol* 2014;**27**:67–72
4. Schmaltz C, Hardenbergh PH, Wells A, Fisher DE. Regulation of proliferation-survival decisions during tumor cell hypoxia. *Mol Cell Biol* 1998;**18**:2845–54
5. Raa A, Stansberg C, Steen VM, Bjerkvig R, Reed RK, Stuhr LE. Hyperoxia retards growth and induces apoptosis and loss of glands and blood vessels in DMBA-induced rat mammary tumors. *BMC Cancer* 2007;**7**:23
6. Holmquist L, Löfstedt T, Påhlman S. Effect of hypoxia on the tumor phenotype: the neuroblastoma and breast cancer models. *Adv Exp Med Biol* 2006;**587**:179–93
7. Axelson H, Fredlund E, Ovenberger M, Landberg G, Påhlman S. Hypoxia-induced dedifferentiation of tumor cells – a mechanism behind heterogeneity and aggressiveness of solid tumors. *Semin Cell Dev Biol* 2005;**16**:554–63
8. Maxwell PH, Dachs GU, Gleadle JM, Nicholls LG, Harris AL, Stratford IJ, Hankinson O, Pugh CW, Ratcliffe PJ. Hypoxia-inducible factor-1 modulates gene expression in solid tumors and influences both angiogenesis and tumor growth. *Proc Natl Acad Sci U S A* 1997;**94**:8104–9
9. Selvendiran K, Kuppusamy ML, Ahmed S, Bratasz A, Meenakshisundaram G, Rivera BK, Khan M, Kuppusamy P. Oxygenation inhibits ovarian tumor growth by downregulating STAT3 and cyclin-D1 expressions. *Cancer Biol Ther* 2010;**10**:386–90
10. Moen I, Tronstad KJ, Kolmannskog O, Salvesen GS, Reed RK, Stuhr LE. Hyperoxia increases the uptake of 5-fluorouracil in mammary tumors independently of changes in interstitial fluid pressure and tumor stroma. *BMC Cancer* 2009;**9**:446
11. Sklizovic D, Sanger JR, Kindwall EP, Fink JG, Grunert BK, Campbell BH. Hyperbaric oxygen therapy and squamous cell carcinoma cell line growth. *Head Neck* 1993;**15**:236–40
12. Plafki C, Peters P, Almeling M, Welslau W, Busch R. Complications and side effects of hyperbaric oxygen therapy. *Aviat Space Environ Med* 2000;**71**:119–24
13. Kallet RH, Matthay MA. Hyperoxic acute lung injury. *Respir Care* 2013;**58**:123–41
14. Arendash GW, Cox AA, Mori T, Cracchiolo JR, Hensley KL, Roberts LJ 2nd. Oxygen treatment triggers cognitive impairment in Alzheimer's transgenic mice. *Neuroreport* 2009;**20**:1087–92
15. Rockswold SB, Rockswold GL, Zaun DA, Zhang X, Cerra CE, Bergman TA, Liu J. A prospective, randomized clinical trial to compare the effect of hyperbaric to normobaric hyperoxia on cerebral metabolism, intracranial pressure, and oxygen toxicity in severe traumatic brain injury. *J Neurosurg* 2010;**112**:1080–94
16. Shi SH, Qi ZF, Luo YM, Ji XM. Normobaric oxygen treatment in acute ischemic stroke: a clinical perspective. *Med Gas Res* 2016;**6**:147–53
17. Shi S, Qi Z, Ma Q, Pan R, Timmins GS, Zhao Y, Shi W, Zhang Y, Ji X, Liu KJ. Normobaric hyperoxia reduces blood occludin fragments in rats and patients with acute ischemic stroke. *Stroke* 2017;**48**:2848–54
18. Ejaz S, Emmrich JV, Sitnikov SL, Hong YT, Sawiak SJ, Fryer TD, Aigbirhio FI, Williamson DJ, Baron JC. Normobaric hyperoxia markedly reduces brain damage and sensorimotor deficits following brief focal ischaemia. *Brain* 2016;**139**(Pt 3):751–64
19. Liu W, Hendren J, Qin XJ, Liu KJ. Normobaric hyperoxia reduces the neurovascular complications associated with delayed tissue plasminogen activator treatment in a rat model of focal cerebral ischemia. *Stroke* 2009;**40**:2526–31
20. Liang Y, Zhong Z, Huang Y, Deng W, Cao J, Tsao G, Liu Q, Pei D, Kang T, Zeng YX. Stem-like cancer cells are inducible by increasing genomic instability in cancer cells. *J Biol Chem* 2010;**285**:4931–40
21. Nikitin AY, Alcaraz A, Anver MR, Bronson RT, Cardiff RD, Dixon D, Fraire AE, Gabrielson EW, Gunning WT, Haines DC, Kaufman MH, Linnoila RI, Maronpot RR, Rabson AS, Reddick RL, Rehm S, Rozengurt N, Schuller HM, Shmidt EN, Travis WD, Ward JM, Jacks T. Classification of proliferative pulmonary lesions of the mouse: recommendations of the mouse models of human cancers consortium. *Cancer Res* 2004;**64**:2307–16
22. Hoogsteen IJ, Marres HA, van der Kogel AJ, Kaanders JH. The hypoxic tumour microenvironment, patient selection and hypoxia-modifying treatments. *Clin Oncol* 2007;**19**:385–96
23. Rockwell S, Dobrucki IT, Kim EY, Marrison ST, Vu VT. Hypoxia and radiation therapy: past history, ongoing research, and future promise. *Curr Mol Med* 2009;**9**:442–58

24. Moen I, Øyan AM, Kalland KH, Tronstad KJ, Akslen LA, Chekenya M, Sakariassen PØ, Reed RK, Stuhr LE. Hyperoxic treatment induces mesenchymal-to-epithelial transition in a rat adenocarcinoma model. *PLoS One* 2009;**4**:e6381
25. Stuhr LE, Raa A, Oyan AM, Kalland KH, Sakariassen PO, Petersen K, Bjerkvig R, Reed RK. Hyperoxia retards growth and induces apoptosis, changes in vascular density and gene expression in transplanted gliomas in nude rats. *J Neurooncol* 2007;**85**:191–202
26. Crapo JD. Morphologic changes in pulmonary oxygen toxicity. *Annu Rev Physiol* 1986;**48**:721–31
27. Davies KJ. Oxidative stress: the paradox of aerobic life. *Biochem Soc Symp* 1995;**61**:1–31
28. Mach WJ, Thimmesch AR, Pierce JT, Pierce JD. Consequences of hyperoxia and the toxicity of oxygen in the lung. *Nurs Res Pract* 2011;**2011**:260482
29. Halliwell B, Gutteridge JM. Role of free radicals and catalytic metal ions in human disease: an overview. *Meth Enzymol* 1990;**186**:1–85
30. Birben E, Sahiner UM, Sackesen C, Erzurum S, Kalayci O. Oxidative stress and antioxidant defense. *World Allergy Organ J* 2012;**5**:9–19
31. Gorrini C, Harris IS, Mak TW. Modulation of oxidative stress as an anticancer strategy. *Nat Rev Drug Discov* 2013;**12**:931–47
32. Panieri E, Santoro MM. ROS homeostasis and metabolism: a dangerous liason in cancer cells. *Cell Death Dis* 2016;**7**:e2253
33. Liu J, Wang Z. Increased oxidative stress as a selective anticancer therapy. *Oxid Med Cell Longev* 2015;**2015**:294303
34. Simon HU, Haj-Yehia A, Levi-Schaffer F. Role of reactive oxygen species (ROS) in apoptosis induction. *Apoptosis* 2000;**5**:415–8
35. Finkel T. Oxidant signals and oxidative stress. *Curr Opin Cell Biol* 2003;**15**:247–54
36. Ott M, Gogvadze V, Orrenius S, Zhivotovsky B. Mitochondria, oxidative stress and cell death. *Apoptosis* 2007;**12**:913–22
37. Jurgensmeier JM, Xie Z, Deveraux Q, Ellerby L, Bredesen D, Reed JC. Bax directly induces release of cytochrome c from isolated mitochondria. *Proc Natl Acad Sci U S A* 1998;**95**:4997–5002
38. Avisetti DR, Babu KS, Kalivendi SV. Activation of p38/JNK pathway is responsible for embelin induced apoptosis in lung cancer cells: transitional role of reactive oxygen species. *PLoS One* 2014;**9**:e87050
39. Wada T, Penninger JM. Mitogen-activated protein kinases in apoptosis regulation. *Oncogene* 2004;**23**:2838–49
40. Ballif BA, Blenis J. Molecular mechanisms mediating mammalian mitogen-activated protein kinase (MAPK) kinase (MEK)-MAPK cell survival signals. *Cell Growth Differ* 2001;**12**:397–408
41. Makena PS, Gorantla VK, Ghosh MC, Bezawada L, Balazs L, Luellen C, Parthasarathi K, Waters CM, Sinclair SE. Lung injury caused by high tidal volume mechanical ventilation and hyperoxia is dependent on oxidant-mediated c-Jun NH2-terminal kinase activation. *J Appl Physiol* 2011;**111**:1467–76
42. Zhu Q, Hu J, Meng H, Shen Y, Zhou J, Zhu Z. S phase cell cycle arrest, apoptosis, and molecular mechanisms of aplasia ras homolog member I-induced human ovarian cancer SKOV3 cell lines. *Int J Gynecol Cancer* 2014;**24**:629–34

(Received January 11, 2018, Accepted April 10, 2018)